Experiment: A chirped fibre grating has been written in a standard SMF-28 telecommunication fibre. The fibre was sensitised by high pressure hydrogen loading [13]. The fibre was placed in a 100atm chamber at room temperature for 10 days. The experimental setup as shown in Fig. 2 was used with a spherical divergent lens of focal length $f = -75$mm situated at a distance $d = 45$mm from the phase mask. The angle α between the fibre and the phase mask was set at 1.6°. The writing source was a Q-switched Nd:YAG laser quadrupled to 266nm. The energy per 10ns pulse was 10mJ and the repetition rate was 9Hz. After 60 min exposure, a 15mm-long chirped fibre grating with the transmission and reflection characteristics presented in Fig. 3*a* was obtained. The background reflection on each side of the resonance peak is due to the Fresnel reflection on the fibre end. The bandwidth of the reflection peak is 6.0nm (FWHM) and agrees well with the value calculated from eqn. 4 which is 5.4nm. As already reported [14], writing a strong grating induces losses at wavelengths shorter than the peak reflectivity wavelength. These losses are due to coupling to the radiation modes. As a result, the reflection characteristics of a strong chirped grating differ depending on the side from which it is interrogated. The curves presented in Fig. 3*a* were recorded with the input signal incident from the shorter period side of the grating. When the interrogating signal was injected from the longer period side, we measured the curves presented in Fig. 3*b* instead.

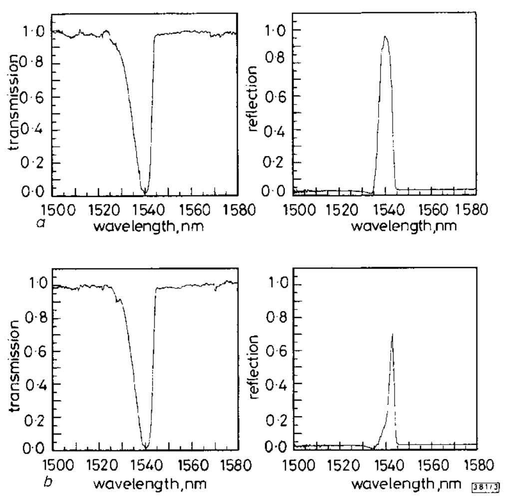

Fig. 3 *Refelction and transmission against wavelength when signal is injected from short period side and from long period side*

a Injected from short period side
b Injected from long period side

Conclusion: By introducing a spherical lens in the well-known phase mask setup and by tilting the fibre from the phase mask, we were able to write a chirped fibre grating with a bandwidth of 6.0nm. The experimental result agrees well with theory. The method is simple, reliable, and compatible with the phase mask method. By choosing different focal length lenses, a large range of chirp magnitude can be obtained in a controlled manner. Assuming a large incident beam on the phase mask (15mm) and reasonable values of f and α (30mm and 10°), a chirped grating with a bandwidth in excess of 100nm could be produced.

18 November 1994

Electronics Letters Online No: 19950110

Y. Painchaud, A. Chandonnet and J. Lauzon (*National Optics Institute, 369 Franquet Street, Sainte-Foy, Quebec G1P 4N8, Canada*)

References

1 MELTZ, G., MOREY, W.W., and GLEN, W.H.: 'Formation of Bragg gratings in optical fibres by a transverse holographic method', *Opt. Lett.*, 1989, **14**, pp. 823–825

2 HILL, K.O., MALO, B., BILODEAU, F., JOHNSON, D.C., and ALBERT, J.: 'Bragg gratings fabricated in monomode photosensitive optical fiber by UV exposure through a phase mask', *Appl. Phys. Lett.*, 1993, **62**, pp. 1035–1037

3 ANDERSON, D.Z., MIZRAHI, V., ERDOGAN, T., and WHITE, A.E.: 'Production of in-fibre gratings using a diffractive optical element', *Electron. Lett.*, 1993, **29**, pp. 566–568

4 OUELLETTE, F.: 'Dispersion cancellation using linearly chirped Bragg grating filters in optical waveguides', *Opt. Lett.*, 1987, **12**, pp. 847–849

5 FARRIES, M.C., SUGDEN, K., REID, D.C.J., BENNION, I., MALONY, A., and GOODWIN, M.J.: 'Very broad reflection bandwidth (44nm) chirped fibre gratings and narrow bandpass filters produced by the use of an amplitude mask', *Electron. Lett.*, 1994, **30**, pp. 891–892

6 KASHYAP, K., MCKEE, P.F., CAMPBELL, R.J., and WILLIAM, D.L.: 'Novel method of producing all fibre photoinduced chirped gratings', *Electron. Lett.*, 1994, **30**, pp. 996–998

7 BYRON, K.C., SUGDEN, K., BRICHENO, T., and BENNION, I.: 'Fabrication of chirped Bragg gratings in photosensitive fibre', *Electron. Lett.*, 1993, **29**, pp. 1659-1660

8 LAUZON, J., THIBAULT, S., MARTIN, J., and OUELLETTE, F.: 'Implementation and characterization of fiber Bragg gratings linearly chirped by a temperature gradient', to be published in *Opt. Lett.*

9 HILL, P.C., and EGGLETON, B.J.: 'Strain gradient chirp of fibre Bragg gratings', *Electron. Lett.*, 1994, **30**, pp. 1172–1174

10 SUGDEN, K., BENNION, I., MOLONY, A., and COPNER, N.J.: 'Chirped gratings produced in photosensitive optical fibres by fibre deformation during exposure', *Electron. Lett.*, 1994, **30**, pp. 440–442

11 HILL, K.O., BILODEAU, F., MALO, B., KITAGAWA, T., THERIAULT, S., JOHNSON, D.C., and ALBERT, J.: 'Aperiodic in-fiber Bragg gratings for optical fiber dispersion compensation'. Tech. Dig. OFC'94, San Jose, 1994

12 PROHASKA, J.D., SNITZER, E., RISHTON, S., and BOEGLI, V.: 'Magnification of mask fabricated fibre Bragg gratings', *Electron. Lett.*, 1993, **29**, pp. 1614–1615

13 LEMAIRE, P.J., ATKINS, R.M., MIZRAHI, V., and REED, W.A.: 'High pressure H_2 loading as a technique for achieving ultrahigh UV photosensitivity and thermal sensitivity in GeO_2 doped optical fibres', *Electron. Lett.*, 1993, **29**, pp. 1191–1193

14 MIZRAHI, V., and SIPE, J.E.: 'Optical properties of photosensitive fiber phase gratings', *J. Lightwave Technol.*, 1993, **LT-11**, pp. 1513–1517

Design of QMF banks using allpass filters

X. Zhang and H. Iwakura

Indexing terms: Digital filters, All-pass filters

The authors consider the design of quadrature mirror filter (QMF) banks using digital allpass filters. The QMF banks consisting of an allpass filter and a pure delay section have an approximately linear phase response, and the phase distortion can be minimised by using another additional allpass filter as an equaliser.

Introduction: QMF banks have received considerable attention because of a wide variety of engineering applications. A common requirement in most applications is that the reconstructed signal should be as close to the input signal as possible. In general, the reconstructed signal suffers from three types of error: aliasing error, amplitude distortion, and phase distortion. One of the purposes of QMF designs is to eliminate these errors. It has been shown [1,2] that the QMF banks composed of two allpass filters can completely eliminate the aliasing error and amplitude distortion. However, no method used to design these QMF banks was explained.

In this Letter, we consider the design of QMF banks composed of a parallel connection of an allpass filter and a pure delay section. By using a pure delay section as one of the subfilters in the parallel structure, we need only design the phase response of another subfilter, allpass filter. Therefore, the analysis and synthesis filters have an approximately linear phase response. Finally, we use another additional allpass filter as an equaliser to minimise the phase distortion.

Design of QMF banks with linear phase responses: A well-known filter bank used in signal coding and communication applications is the QMF bank. It has been shown [1, 2] that if the analysis filters $H_0(z)$ and $H_1(z)$ of the QMF bank are composed of a parallel interconnection of two allpass filters,

$$\begin{cases} H_0(z) = \frac{1}{2}[A_N(z^2) + z^{-1}A_M(z^2)] \\ H_1(z) = \frac{1}{2}[A_N(z^2) - z^{-1}A_M(z^2)] \end{cases} \quad (1)$$

where $A_N(z)$, $A_M(z)$ are Nth and Mth order digital allpass functions respectively, and the synthesis filters $F_0(z)$ and $F_1(z)$ satisfy the relations

$$\begin{cases} F_0(z) = H_0(z) \\ F_1(z) = -H_1(z) \end{cases} \quad (2)$$

then the aliasing errors can be completely eliminated. With the aliasing errors removed, the QMF bank becomes a linear and shift-invariant system with the transfer function

$$T(z) = \frac{1}{2}z^{-1}A_N(z^2)A_M(z^2) \quad (3)$$

which is allpass, and there is no amplitude distortion. Hence we need only consider the design of the analysis filters $H_0(z)$ and $H_1(z)$ and the elimination of the phase distortion of $T(z)$.

To obtain QMF banks with linear phase responses, we replace $A_M(z)$ by a pure delay section z^{-M} in eqn. 1; then $H_0(z)$ and $H_1(z)$ become

$$H_{0,1}(z) = \frac{1}{2}[A_N(z^2) \pm z^{-(2M+1)}] \quad (4)$$

The structure of the QMF bank is shown in Fig. 1; a total of N multipliers are needed to implement both $H_0(z)$ and $H_1(z)$. Assume that the phase response of $A_N(z)$ is $\varphi(\omega)$, the frequency responses of $H_0(z)$ and $H_1(z)$ are then given by

$$\begin{cases} H_0(e^{j\omega}) = \exp\left\{j\frac{\varphi(2\omega) - (2M+1)\omega}{2}\right\} \\ \qquad \times \cos\frac{\varphi(2\omega) + (2M+1)\omega}{2} \\ H_1(e^{j\omega}) = j\exp\left\{j\frac{\varphi(2\omega) - (2M+1)\omega}{2}\right\} \\ \qquad \times \sin\frac{\varphi(2\omega) + (2M+1)\omega}{2} \end{cases} \quad (5)$$

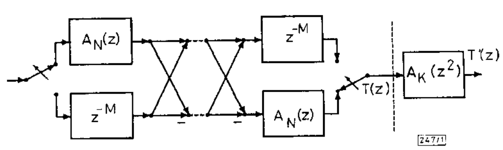

Fig. 1 *Structure of QMF bank using allpass filters*

For a stable allpass filter, its phase is 0 when $\omega = 0$, $-N\pi$ when $\omega = \pi$, and it is required to decrease monotonically with increasing frequency. Therefore, $H_0(z)$ is a lowpass filter, and $H_1(z)$ is a highpass filter. The order of $A_N(z)$ must be chosen as $N = M$ or $N = M + 1$. To obtain a lowpass-highpass filter pair, the desired phase response $\varphi_d(2\omega)$ of $A_N(z^2)$ must be

$$\varphi_d(2\omega) = \begin{cases} -(2M+1)\omega & (0 \le \omega \le \omega_p) \\ -(2M+1)\omega \pm \pi & (\omega_s \le \omega \le \pi) \end{cases} \quad (6)$$

where ω_p, ω_s are band-edge frequencies of $H_0(z)$ in the passband and stopband, respectively, $\omega_p + \omega_s = \pi$. Therefore, it can be seen from eqn. 5 that the phase responses of $H_0(z)$ and $H_1(z)$ will become linear within its passband and stopband regions. By simplifying eqn. 6, we obtain

$$\varphi_d(\omega) = -\left(M + \frac{1}{2}\right)\omega \quad (0 \le \omega \le 2\omega_p) \quad (7)$$

Hence design of the analysis filters with linear phase responses are reduced to a phase design of the allpass filter $A_N(z)$. Let δ_A be the phase error of $A_N(z)$; the phase errors of $H_0(z)$ and $H_1(z)$ are half the phase error of $A_N(z)$, i.e. $\delta_p = \delta_A/2$. The passband and stopband magnitude errors of $H_0(z)$ and $H_1(z)$ are $\Delta_{0p} = 1 - \cos(\delta_A/2) \simeq \delta_A^2/8$, $\Delta_{0s} = \sin(\delta_A/2) \simeq \delta_A/2$, $\Delta_{1p} = \Delta_{0p}$, and $\Delta_{1s} = \Delta_{0s}$, respectively. In most cases, the selection $N = M + 1$ can give smaller errors than $N = M$. In [5], we proposed a new method for designing digital allpass filters. By using the proposed method, we can design $A_N(z)$ with an equiripple phase response, hence the equiripple magnitude and phase responses of the analysis filters can be obtained simultaneously.

Elimination of phase distortion: From eqn. 3, the overall transfer function of the QMF bank is

$$T(z) = \frac{1}{2}z^{-(2M+1)}A_N(z^2) \quad (8)$$

which is allpass, and the phase response is dependent on the phase response of $A_N(z)$. It is seen from eqn. 7 that although $\varphi(\omega)$ is linear within the region $[0, 2\omega_p]$, the phase response of $T(z)$ is nonlinear in the entire frequency regions because $\varphi(\omega)$ cannot be approximated to be linear in the transition band $[2\omega_p, \pi]$. Hence we use another additional allpass filter $A_K(z^2)$ as an equaliser to compensate the phase response of $T(z)$. The total transfer function becomes

$$T'(z) = T(z)A_K(z^2) = \frac{1}{2}z^{-(2M+1)}A_N(z^2)A_K(z^2) \quad (9)$$

To force $T'(z)$ to have a linear phase at all frequencies, after considering the stable conditions of allpass filters, we have

$$A_N(z)A_K(z) = z^{-(N+K)} \quad (10)$$

and then the desired phase response $\theta_d(\omega)$ of $A_K(z)$ is

$$\theta_d(\omega) = -(N+K)\omega - \varphi(\omega) \quad (0 \le \omega \le \pi) \quad (11)$$

where $\varphi(\omega)$ is the actual phase response of the designed allpass filter $A_N(z)$. The order K of $A_K(z)$ is decided by the specification of phase distortion of $T'(z)$. Therefore, the design problem of the QMF banks with linear phase responses becomes the phase design of two allpass filters $A_N(z)$ and $A_K(z)$.

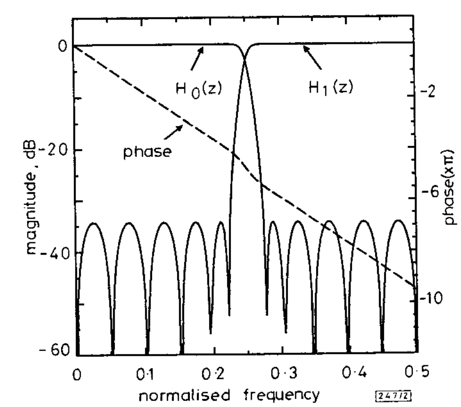

Fig. 2 *Frequency responses of analysis filters*

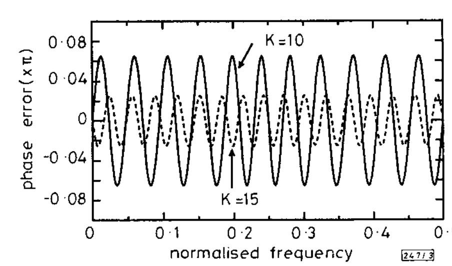

Fig. 3 *Phase errors of total transfer function*

——— $K = 10$
– – – – $K = 15$

Design example: The aim is to design a QMF bank with the following specification: $N = 5$, $M = 4$, $\omega_p = 0.45\pi$ and $\omega_s = 0.55\pi$. We use the procedure proposed in [5] to design two allpass filters $A_N(z)$ and $A_K(z)$. The frequency responses of the analysis filters $H_0(z)$ and $H_1(z)$ are shown in Fig. 2. In Fig. 2, the solid curve indicates the magnitude responses, and the broken curve indicates the phase response. It is seen that equiripple magnitude and phase responses have been obtained. The phase errors of the total transfer function are shown in Fig. 3. The phase responses are equiripple.

Conclusion: We have proposed a procedure for designing QMF banks using allpass filters. By using a pure delay section as one of the subfilters in the parallel structure, we only need to design an allpass filter to obtain the analysis and synthesis filters with approximately linear phase responses, and use another additional allpass filter as an equaliser to minimise the phase distortion of the total transfer function.

7 November 1994
Electronics Letters Online No: 19950097

X. Zhang and H. Iwakura (*Department of Communications and Systems, University of Electro-Communications, 1-5-1 Chofugaoka, Chofu-shi, Tokyo 182, Japan*)

References

1 VAIDYANATHAN, P.P., REGALIA, P.A., and MITRA, S.K.: 'Design of doubly complementary IIR digital filters using single complex allpass filter, with multirate applications', *IEEE Trans.*, 1987, **CAS-34**, pp. 378–389
2 REGALIA, P.A., MITRA, S.K., and VAIDYANATHAN, P.P.: 'The digital allpass filter: a versatile signal processing building block', *Proc. IEEE*, 1988, **76**, pp. 19–37
3 KIM, C.W., and ANSARI, R.: 'Approximately linear phase IIR filters using allpass sections'. Proc. ISCAS-1986, 1986, pp. 661–664
4 RENFORS, M., and SARAMÄKI, T.: 'A class of approximately linear phase digital filters composed of allpass subfilters'. Proc. ISCAS-1986, 1986, pp. 678–681
5 ZHANG, X., and IWAKURA, H.: 'Novel method for designing digital allpass filters based on eigenvalue problem', *Electron. Lett.*, 1993, **29**, pp. 1279–1281

Image vector quantisation using a modified LBG algorithm with approximated centroids

H.A. Monawer

Indexing terms: Image processing, Vector quantisation

A new image vector quantiser (VQ) is introduced which uses a modified LBG algorithm for codebook production called LBG with approximated centroids (LBG-AC). Simulations show that an increase in PSNR (~0.7–1.2dB) can be achieved using VQ with the LBG-AC algorithm over VQ with the LBG algorithm.

Introduction: Image data compression has been an active area of research for many years. A fundamental goal of image data compression is to reduce the bit rate for transmission or data storage while maintaining all acceptable fidelity or image quality. Vector quantisation (VQ) has proven to be an effective technique for encoding speech and images, especially at low bit rates. It can be used in TV broadcasting, video conferencing, and the storage of pictures in databases etc.

Vector quantisation: The key step in VQ [1, 2] is to generate a good codebook from a training set. The K-means algorithm proposed by Linde *et al.* (denoted as the LBG algorithm) [1], is typically used to generate the codebook. However, a direct VQ applied to images has a very simple hardware structure but the reconstructed VQ images suffer from two major problems: visible block structure, and edge degradation [3]. The main reason for the appearance of these problems is attributed to the fact that the code vectors in the LBG algorithm are produced by taking the average of all blocks in the cluster, which results in edge degradation within the blocks quantised using these code vectors. To reduce the above mentioned problems we propose a new algorithm for codebook production. This algorithm is an LBG algorithm with post-processing of the output centroids at each iteration. We called this algorithm LBG with approximated centroids (LBG-AC).

LBG-AC algorithm: The LBG-AC algorithm is an LBG algorithm follwed by a specific approximation of the centroids at each iteration. The approximation means the replacement of the centroids at each iteration by vectors taken from the training set in such a way that the quality of the output code vectors is improved. Here, we consider the following modifications of the LBG-AC algorithm:

(i) In the first case, each centroid at each iteration is replaced by the closest vector (taken from the training set) that minimises the MSE, i.e the nearest neighbour to the required centroid. The search for the nearest neighbour is carried over all vectors in the training set. We called this modification LBG-AC with full approximation search (LBG-AC-FAS).

(ii) In the second case, we take into account the error associated with the approximation. In other words, if the MSE between the centroid and its approximation is less than a threshold, then the approximation is implemented; otherwise, the centroid will not be replaced and no approximation is implemented. We called this modification LBG-AC with full thresholded approximation search (LBG-AC-FTAS).

(iii) To reduce the computational cost required for the approximation process, the search for the nearest neighbour of each centroid can be carried over a part of the training set. This means that the approximation is to be choosen from the cluster used in performing the required centroid, i.e. the centroid will be replaced by the closest vector within the corresponding cluster. We call this modification LBG-AC with local approximation search (LBG-AC-LAS).

(iv) Here, the difference from the previous case, case (iii), is that the approximation will be implemented if the MSE between the centroid and its local approximation is less than a threshold. We called this modification LBG-AC with local thresholded approximation search (LBG-AC-LTAS).

To prove our consideration, suppose that Y is the centroid of the cluster C_j at the current iteration, X_k is the approximation of Y and θ^2 is the threshold (in (ii) and (iv)).We can then write

$$|X_k - Y| = \theta \tag{1}$$

After approximation, the MSE in the cluster C_j

$$d(X, X_k) = \frac{1}{n} \sum_{x_i \in C_j} (x_i - X_k)^2 \tag{2}$$

where x_i is the ith vector in the cluster C_j and n is the number of vectors in C_j.

Substituting eqn. 1 into eqn. 2 and applying same algebraic manipulations, we have

$$d(X, X_k) = \frac{1}{n} \sum_{x_i \in C_j} (x_i - Y)^2 - \frac{2\theta}{n} \sum_{x_i \in C_j} |x_i - Y| + \theta^2 \tag{3}$$

Note that the last two terms in eqn. 3 correspond to the error associated with selecting the approximation X_k instead of the centroid Y. Relative to the actual value (first term in eqn. 3), the error of the approximation is small with respect to the advantage of using the LBG-AC algorithm in preserving the edges.

Simulation results: In this Section we examine the performance of the LBG-AC algorithm on a variety of monochrome images. All these images had 256 × 256 pixels and 8 bit/pixel resolution. Here, several objective measures of the performance evaluations are used such as: mean squared error (MSE), peak SNR (PSNR) and the normalised computational time (NCT) required to produce the output codebook.